Sea surface drag and the role of spray

David H. Richter[1] and Peter P. Sullivan[1]

Received 20 December 2012; accepted 14 January 2013; published 11 February 2013.

[1] Motivated by the possible effects of spray on the drag felt by the ocean surface in high winds, we use direct numerical simulation coupled with Lagrangian particle tracking to investigate how suspended inertial particles alter momentum flux in an idealized turbulent flow. Turbulent Couette flow is used for this purpose since the momentum flux profile is constant across the domain height; a characteristic similar to the constant-flux layer in the atmospheric surface layer. The simulations show that when inertial particles are introduced into a turbulent flow, they carry a portion of the total vertical momentum flux, and that this contribution can be significant when the particle concentration is sufficiently large. The numerical setup is also used to evaluate a dispersed phase model that treats spray effects as equivalent to an increase in stable atmospheric stratification. Our simulations suggest that in the range of droplet sizes typically found near the air-sea interface, particle inertial effects dominate any particle-induced stratification effects. **Citation:** Richter, D. H., and P. P. Sullivan (2013), Sea surface drag and the role of spray, *Geophys. Res. Lett.*, *40*, 656–660, doi:10.1002/grl.50163.

1. Introduction

[2] The behavior of surface drag with increasingly high winds over the ocean is an important piece of information for making accurate hurricane predictions, while at the same time a subject of debate within both the atmosphere and ocean science communities. The source of debate involves the parameterization of the surface stress through a drag coefficient C_D, varying with wind speed commonly measured at a reference height of 10 m:

$$\tau = \rho_f C_D U_{10}^2 \tag{1}$$

[3] Here τ is the total stress at the surface, or equivalently the amount of horizontal momentum being transferred vertically to the surface from the winds above. ρ_f is the density of the air, U_{10} is the mean velocity at the 10 m height, and C_D is the drag coefficient.

[4] Early parameterizations, such as that by *Large and Pond* [1981], are based on a linear relationship between C_D and U_{10}, obtained by fitting various field observations and laboratory measurements. These parameterizations, however, are only valid up to 20–25 m/s, and when extrapolated to higher winds predict unrealistic values of the ratio C_K/C_D, where C_K is the bulk transfer coefficient for enthalpy flux at the surface [*Emanuel*, 1995]. More recently, measurements and observations at higher wind speeds confirm that the surface drag coefficient indeed saturates or even decreases at hurricane-force winds [*Powell et al.*, 2003; *Donelan et al.*, 2004; *Bell et al.*, 2012], which has led to a search for an explanation for such behavior.

[5] Sea spray is commonly invoked as an explanation for the saturation of drag coefficient at high winds, where spray is injected into the near-surface boundary layer through both breaking waves and spume torn from wave crests. One line of thought is that spray acts by altering the local effective density, providing a buoyancy force which acts as a sink of turbulent kinetic energy, analogous to thermal buoyancy in a stably stratified fluid layer. This idea has its origins in theory aimed at explaining dusty flows [*Barenblatt and Golitsyn*, 1974] and has led to several modeling attempts which account for spray through a modification of the turbulent kinetic energy budget [*Barenblatt et al.*, 2005; *Kudryavtsev*, 2006; *Bao et al.*, 2011]. A second line of thought considers the more direct effect which spray has on the air momentum or energy kinetic energy budgets, by including feedbacks such as adding a momentum source due to spray [*Kudryavtsev and Makin*, 2011], or splitting up contributions between spray and air to the total stress [*Andreas*, 2004] or the total kinetic energy [*Pielke and Lee*, 1991]. A third line of thought is that spray is not responsible for the saturation of surface drag coefficient. Other processes, such as changes in surface aerodynamic roughness [*Mueller and Veron*, 2009; *Andreas et al.*, 2012], are responsible for the saturation or reduction of C_D.

[6] The current letter is based on a different approach compared to previous investigations of sea spray. Here we use the results of *Richter and Sullivan* [in review] (referred to as "RS" throughout) to relate an idealized study of inertial particles in wall-bounded turbulent flow to the physical mechanisms underlying the interaction of spray with near-surface winds. By tracking individual Lagrangian particles in turbulent Couette flow and explicitly coupling the momentum exchanged between the air and particle phases, our work aims to describe in what ways particles (such as sea spray) can modify a turbulent flow. Note that we do not claim to simulate sea spray and all of its accompanying physical processes, such as spray generation or wave breaking, directly. Rather, we perform direct numerical simulation of an idealized turbulent flow to find the conditions under which a dispersed phase of dense particles can modify the surrounding turbulence in ways suggested by the aforementioned spray models.

2. Numerical Setup

[7] Details of the numerical method and its validation can be found in RS, and only a brief summary is given here. Direct numerical simulation (DNS—i.e., all scales of turbulent

[1]National Center for Atmospheric Research, Boulder, Colorado, USA.

Corresponding author: D. H. Richter, National Center for Atmospheric Research, PO Box 3000, Boulder, CO, 80307, USA. (drichter@ucar.edu)

0094-8276/13/10.1002/grl.50163

motion are resolved on the computational mesh) of turbulent Couette flow is performed while simultaneously tracking the trajectories of many (up to four million) Lagrangian point-particle elements designed to represent spray particles in air. At the start of a given simulation, the particles are initialized with a uniform concentration throughout the domain, and their initial velocity is set equal to the carrier phase velocity at the initial position. Particles collide elastically with the upper and lower walls. The particles are inertial, and their trajectory is dictated by the viscous drag of the surrounding fluid, computed from the Stokes drag on a solid sphere. As a single particle is accelerated by the surrounding fluid, this process implies an exchange of momentum between the carrier phase (the air) to the dispersed phase (the particle). Therefore, the force which a particle feels through the surrounding viscous drag is fed back as a force with opposite sign in the carrier phase momentum equations. This setup is then used to study the changes in turbulence and momentum transfer with varying particle characteristics.

[8] The particles represented in the simulations are assumed to be smaller than the Kolmogorov turbulence length scale, and the particle volume fraction is assumed small so that particle-particle interactions can be ignored. The equations solved are the incompressible Navier-Stokes equations for the carrier phase, neglecting thermal buoyancy, using only a molecular viscosity (i.e., no sub-grid diffusivity), and including a feedback force to represent momentum coupling between phases.

[9] Turbulent Couette flow is simulated, which develops between two infinitely parallel plates moving in equal and opposite directions (see Figure 1).

[10] This geometry is chosen because the total carrier phase stress in the wall-normal direction is constant—a characteristic similar to the constant-flux layer of the atmospheric boundary layer, which also allows for unambiguous comparisons of momentum flux budgets with and without the presence of spray. The Reynolds number is defined as $Re = U_0 H/\nu_f$, where U_0 is the difference in plate velocity, H is the plate separation distance, ν_f is the kinematic viscosity of air, and $Re = 8100$ throughout this study.

[11] In non-dimensional form, the equations governing the evolution and feedback of the particles are influenced primarily by the particle Stokes number and the mass fraction of the dispersed phase. The particle Stokes number, defined as $St_K = \tau_p/\tau_K$, is the ratio of the particle acceleration time scale τ_p and the Kolmogorov time scale of the turbulence τ_K at the channel mid-height. Physically, the Stokes number indicates how easily turbulent motions at the Kolmogorov length scale can change the trajectory of a particle. Zero St_K implies passive tracers, where the particles can instantaneously adjust to the surrounding flow velocity, while the limit of infinite St_K implies ballistic particles,

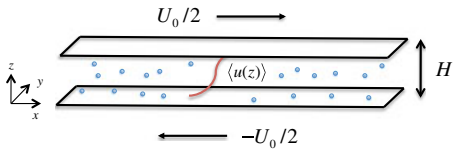

Figure 1. Schematic of Couette cell geometry. Reference velocity U_0 is the difference in plate velocity and reference length H is the distance between the plates. Example mean velocity profile is shown in red.

whose trajectories are not influenced by the surrounding flow. The mass fraction, φ_m, is defined as the ratio of total dispersed phase mass to total carrier phase mass in the entire domain. For water in air, where the ratio of the densities ρ_p (the particle density) and ρ_f (the carrier phase density) is approximately 1000, φ_m can be large while still maintaining a small volume fraction of particles.

3. Results

[12] In our recent study (RS), we describe how turbulence statistics change with increasing dispersed phase mass φ_m or increasing particle inertia St_K. Presently, we interpret these results in the context of spray loading near the air-sea interface. As shown in RS, a horizontally averaged momentum budget across the Couette flow geometry leads to the following definition for the total stress:

$$\tau = \rho_f \left\langle u' w' \right\rangle - \rho_f \nu_f \frac{\partial U}{\partial z} - \int_0^z \langle F_x(z^*) \rangle dz^* = \tau_{\text{turbulent}} + \tau_{\text{viscous}} + \tau_{\text{particle}}. \quad (2)$$

[13] The total stress τ is the value of the total momentum transferred from the bottom to the top plate. The first and second terms on the right-hand side are the turbulent momentum flux and the viscous stress, respectively. The third term involves a vertical integral of the average horizontal particle feedback force F_x and represents the momentum being transferred in the vertical direction by the dispersed phase. From a momentum balance of the dispersed phase, this particle stress (denoted τ_{particle} throughout) can be shown to be equivalent to the mass-weighted "turbulent stress" of the dispersed phase:

$$\tau_{\text{particle}} = \int_0^z -\langle F_x(z^*) \rangle dz^* = \rho_p \langle c \rangle \left\langle u'_p w'_p \right\rangle_c. \quad (3)$$

[14] Here, c is the instantaneous particle volume concentration, u'_p and w'_p are the fluctuating streamwise and wall-normal particle fluctuating velocities, and $\langle \cdot \rangle_c$ refers to an average taken over the dispersed phase.

[15] In this context, eddy flux measurements such as those collected in the CBLAST campaign [*French et al.*, 2007] directly measure the turbulent stress, denoted $\tau_{\text{turbulent}}$ throughout this work. On the other hand, stresses deduced as the residual of an integral momentum balance such as in *Bell et al.* [2012] presumably yield the total stress, since they implicitly include all forms of momentum transport.

[16] Several cases are chosen to probe the parameter space of φ_m and St_K. At $St_K = 10$ (the acceleration time scale of the particles is 10 times the Kolmogorov time scale), the mass fraction is varied between $\varphi_m = [0.1, 0.25, 0.5]$. Then, at $\varphi_m = 0.25$ (the total mass of the dispersed phase in the domain is 25% of the carrier phase mass), the Stokes number is varied as $St_K = [O(1), O(10), O(100)]$. The details behind these cases and their effects on the turbulence can be found in RS.

[17] Figure 2a plots the distribution of the stress components across the domain height for all cases, including an unladen case. The height is non-dimensionalized by H, and the values of stress are made dimensionless with $\rho_f U_0^2$.

[18] Figure 2a shows that under certain conditions, the turbulent stress can be significantly reduced from its unladen value. This behavior increases monotonically as the mass

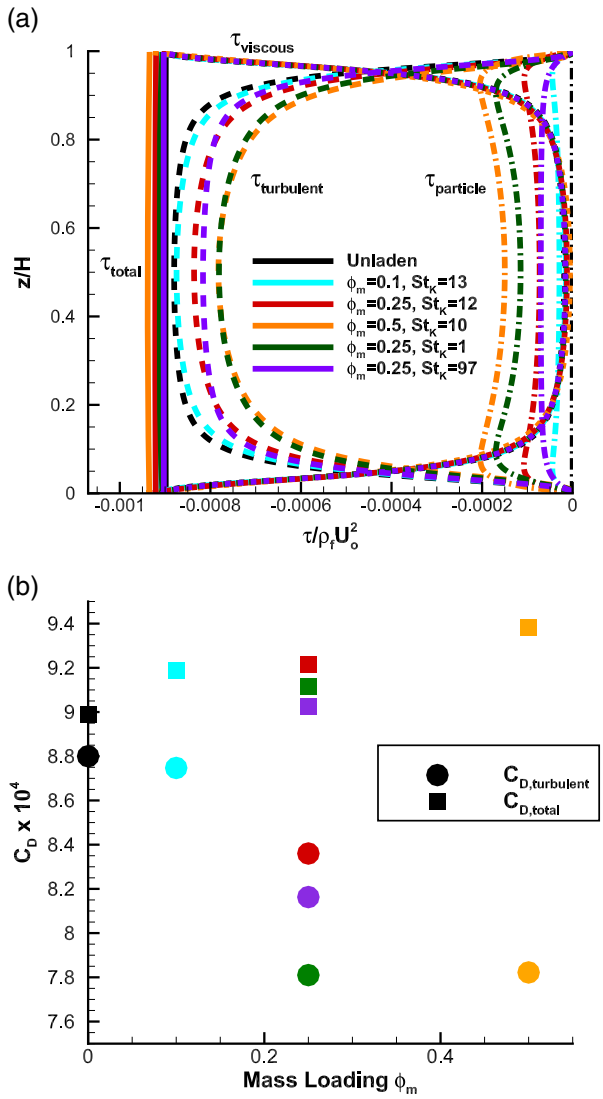

Figure 2. (a) Profiles of total stress (solid), turbulent stress (dashed), viscous stress (dotted), and particle stress (dash-dotted) as a function of domain height. Height normalized by H and stress normalized by $\rho_f U_0^2$. (b) Variation of the drag coefficients based on the total stress, $C_{D,\text{total}}$ (squares), and the turbulent stress, $C_{D,\text{turbulent}}$ (circles), as a function of mass fraction φ_m.

loading of the dispersed phase is increased, and is maximized at $St_K \approx 1$. From the plot, however, it is clear that this does not necessarily imply a reduction in the total stress, as the particle stress τ_{particle} nearly exactly compensates for the loss in turbulent stress. Therefore, despite a maximum 15% reduction in $\tau_{\text{turbulent}}$, the total stress τ_{total} remains unchanged within 5%.

[19] In RS it is argued that the reduction of $\tau_{\text{turbulent}}$ is due to a weakening or complete suppression of near-wall vortical motions which are responsible for turbulent momentum transfer in a wall-bounded flow. If an inertial spray particle enters a vortex, the drag associated with accelerating that particle appears as a counter-torque for the motion of the vortex, thus weakening it. The weakening of near-wall coherent structures leads to a reduction in the correlation $\langle u'w' \rangle$.

[20] From these momentum flux components, one can define a drag coefficient using U_0 as a velocity scale and the values of the stresses at the domain mid-height. This is analogous to making a flux measurement at some point well above the viscous layer. The only question, however, is which value of stress to use:

$$C_{D,\text{total}} = \frac{\tau_{\text{total}}}{\rho_f U_0^2}, \tag{4}$$

or

$$C_{D,\text{turbulent}} = \frac{\tau_{\text{turbulent}}}{\rho_f U_0^2}. \tag{5}$$

[21] Figure 2b shows both definitions of C_D versus the particle mass fraction φ_m. Circles indicate C_D based on the turbulent stress (equation (5)) and squares are based on the total stress (equation (4)). As noted above, the reduction in $\tau_{\text{turbulent}}$ is monotonic with spray mass loading, and a drag coefficient defined by (5) then decreases. The drag coefficient based on the total stress, however, remains nearly constant and even increases slightly with φ_m.

4. Interpretation

[22] In the atmosphere, the results of the previous section imply that a measurement of the turbulent flux $\tau_{\text{turbulent}} = \rho_f \langle u'w' \rangle$ at some height within the spray layer underestimates the total stress that the bottom surface is experiencing. This is exactly what *Andreas* [2004] argues, that near the air-sea interface spray can carry a significant portion of the total stress, which itself remains constant with height immediately above the surface. A comparison of Figure 2b to Figure 6 of *Andreas* [2004] leads to a similar conclusion: the drag coefficient based only on the turbulent momentum flux appears to decrease despite C_D based on the total stress behaving differently (note that *Andreas* [2004] plots U_{10} on the abscissa; here, the mass fraction can be viewed as a rough surrogate for U_{10} since spray concentrations increase with wind speed).

[23] In the spray-laden boundary layer above the ocean surface, one can, in principle, express the total stress as the sum of the viscous, turbulent, and spray components, as equation (2) is merely a mathematical definition. Despite disparities between our idealized numerical setup and the atmospheric spray-laden boundary layer, we argue that the same qualitative behavior will be seen, particularly as the spray mass loading increases. If eddy-flux measurements are taken above the spray layer, then the turbulent stress likely represents the total stress well. Likewise, if eddy-flux measurements are made within the spray layer, the measured stress only represents the total stress if the mass loading of the particles is sufficiently small. At this point it should be noted that the values of φ_m used in this study are not chosen to match observed quantities, since accurately measuring spray concentration is notoriously difficult in the high-wind, near-surface boundary layer. Instead, these values are chosen to identify the level at which spray begins to alter the momentum transfer budget.

[24] It is therefore important to consider measurements such as those done by *Donelan et al.* [2004], who compare direct measurements of $\langle u'w' \rangle$ with other inferred measurements of the stress through global momentum budgets. The agreement of the explicit measurements in *Donelan et al.* [2004] with the stress based on global momentum balances indicates that the spray stress as defined in equation (3) is

negligibly small in their laboratory setup, which then leads to the conclusion that spray is not likely the cause of the drag coefficient saturation. This is in agreement with several studies, such as that by *Andreas et al.* [2012] and *Holthuijsen et al.* [2012], which point to aerodynamic effects as the root cause of the saturation of C_D.

5. Gravity

[25] A common approach to modeling the effect of sea spray is to treat spray as a change in stratification of the near-surface layer [*Makin*, 2005; *Kudryavtsev*, 2006; *Barenblatt et al.*, 2005] through its modification of the effective mixture density. As outlined in *Barenblatt and Golitsyn* [1974], the assumptions behind this model are that the particle Stokes number and the particle volume fraction are very small. Furthermore, deviations of the mixture density from the unladen air density are small so that the Boussinesq approximation can be applied.

[26] In the simulations described in the previous sections, the particles feel no gravitational force. Therefore, for the purpose of investigating the theory of *Barenblatt and Golitsyn* [1974] in the present framework, gravity is applied to the particles in the wall-normal direction. When a particle reaches the bottom wall of the domain, it is reintroduced at a random location along the bottom surface with zero horizontal velocity and a wall-normal (upwards) velocity uniformly distributed between 0 and $U_0/2$. The gravitational body force on each particle is chosen to ensure that the ratio of the particle terminal velocity to the Kolmogorov velocity scale, $V_g/v_k = 0.4$. At $\varphi_m = 0.05$, three different Stokes numbers of $St_K = [O(0.1), O(1.0), O(10.0)]$ are chosen to probe how particles of non-zero Stokes number behave relative to the particle-induced stratification theory. Namely, we are testing whether or not the effects on turbulence caused by the dispersed phase can be explained by changes in the effective mixture density.

[27] A turbulent kinetic energy (TKE) budget derived from the fluid momentum equations using the Boussinesq approximation for a horizontally homogeneous flow has a buoyancy production term of the form $\langle \rho' w' \rangle g$, where g is gravitational acceleration. Here, ρ refers to fluctuations of the total density, which in the presence of a dispersed phase is solely a function of the particle concentration: $\rho = \rho_f(1-c) + \rho_p c$, where c is the instantaneous volume concentration of particles, ρ_f is the air density, and ρ_p is the particle density. Substituting this expression into the buoyancy production term results in a total TKE budget of the form:

$$-\rho_f \left\langle u' w' \right\rangle \frac{\partial \langle u \rangle}{\partial z} - \left\langle c' w' \right\rangle g \left(\rho_p - \rho_f \right) + T - \varepsilon = 0, \qquad (6)$$

where T is TKE transport and ε is TKE dissipation.

[28] Rather than containing a buoyancy term, the current numerical formulation includes a direct particle feedback force F_i in the fluid momentum equations. This leads to a TKE budget which instead has the form:

$$-\rho_f \left\langle u' w' \right\rangle \frac{\partial \langle u \rangle}{\partial z} + \left\langle u'_i f'_i \right\rangle + T - \varepsilon = 0, \qquad (7)$$

where f'_i is the fluctuating feedback force (summation over index i implied).

[29] Figure 3 shows the various terms in the TKE budget varying over the domain height.

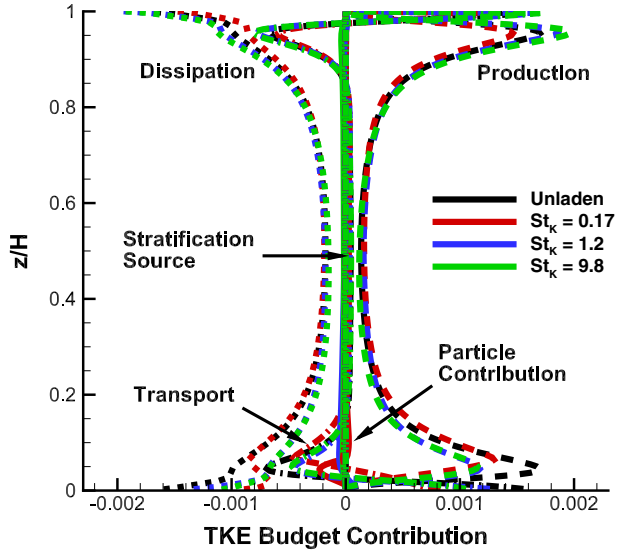

Figure 3. Terms of the TKE budget over the domain height for $St_K = [0.17, 1.2, 9.8]$. Colors corresponding to various St_K indicated in the legend. Lines are as follows: production (dashed), dissipation (dotted), transport (dash-dotted), particle contribution (solid), and particle-induced stratification (dash-double-dotted). Terms non-dimensionalized by $\rho_f U_0^3 / H$

[30] In the figure, the "true" particle contribution (second term in equation (7)) is plotted with solid lines while that computed from the Boussinesq approximation (second term in equation (6)) is plotted with dash-double-dotted lines. These terms are clearly small in magnitude relative to the other terms in the TKE budget. Rather than responding as if the dispersed phase acts as a sink of TKE, the flow adjusts in a way which is manifested as a reduction in TKE production and dissipation (and to a lesser extent transport), highlighting a more complicated interaction between the phases.

[31] Furthermore, it is interesting to note that since the particles are injected from the bottom, gradients of particle concentration vary from small to large among the three runs as St_K is decreased. When $St_K = 0.17$, for example, the value of ρ/ρ_f varies from 1 to 2 in the lower half of the domain—a range quite large compared to, for instance, density fluctuations resulting from typical atmospheric thermal fluctuations. Despite this large density gradient, the TKE source due to particle-induced stratification is, at its highest value, still an order of magnitude less than the source due to momentum coupling between the phases. As noted above, however, even this momentum coupling source is small compared to reductions of TKE production. The changes in production and dissipation are themselves due to the modification of $\langle u'w' \rangle$ which arise from particle drag—a mechanism quite difficult to represent by a change in density stratification.

[32] One of the key approximations in *Barenblatt and Golitsyn* [1974] is that the suspended dispersed phase is assumed to have a very small Stokes number. Clearly our St_K does not match this criterion. Even the $St_K = 0.17$ case exhibits a small degree of inertial effects, such as particle clustering (not shown). In the spray-laden boundary layer above the air/sea interface, it is therefore important to consider the range of Stokes numbers of the particles suspended by turbulence. The theory developed in *Barenblatt and Golitsyn*

[1974] is applicable to dust storms, where dust particle diameters are typically of the order 1 μm or less ($St_K \lesssim O(10^{-4})$ using the same estimation described below). Spray droplet radii, however, can range anywhere from roughly O(10 μm) to O(1000 μm) [*Fairall et al*., 2009]. As a rough (conservative) approximation, if the Kolmogorov length scale of the near-surface turbulence is $\eta_K \approx 1$ mm, this leads to a range of $0.02 \leq St_K \leq 220$ in particle Stokes numbers. The large Stokes numbers present in the spray-laden flow above the surface therefore suggest that a mechanical feedback, namely where particle drag, due to the particle inertia, directly acts on turbulent air fluctuations. This is then responsible for changes observed in the turbulence, rather than a TKE damping effect due to enhanced stable stratification.

6. Conclusions

[33] Idealized turbulence simulations show that turbulent momentum flux $\rho_f \langle u'w' \rangle$ is reduced in wall-bounded flows for sufficiently high concentrations of inertial particles. Supplementing this loss of turbulent flux, however, is an additional momentum flux carried by the dispersed phase, which leads to a total momentum flux that remains roughly constant. This suggests that when measurements of $\langle u'w' \rangle$ are made to estimate surface stress in high winds, the potential exists to miss a portion of the total flux, which leads to an underestimate of the value of C_D. Studies which corroborate eddy flux correlations using global momentum budgets and still show reductions of C_D in high wind speeds suggest that momentum carried by the dispersed phase is small, indicating that spray is not responsible for the saturation of surface drag coefficient. Furthermore, the simulations are used to investigate the role of particle-induced density stratification on momentum transport. Since the theory of *Barenblatt and Golitsyn* [1974] assumes a very small particle Stokes number, we find that particle drag, rather than density stratification, is responsible for changes in turbulent kinetic energy and momentum flux inflows with a dispersed phase of $St_K \geq 0.1$.

[34] **Acknowledgments.** The authors would like to acknowledge the National Science Foundation, which sponsors the National Center for Atmospheric Research, as well as the Advanced Study Program within NCAR for postdoctoral support.

References

Andreas, E. (2004), Spray stress revisited, *J. Phys. Oceanogr.*, *34*, 1429–1440.

Andreas, E. L., L. Mahrt, and D. Vickers (2012), A new drag relation for aerodynamically rough flow over the ocean, *J. Atmos. Sci.*, *690*(8), 2520–2537, doi:10.1175/JAS-D-11-0312.1.

Bao, J.-W., C. W. Fairall, S. A. Michelson, and L. Bianco (2011), Parameterizations of sea-spray impact on the air-sea momentum and heat fluxes, *Monthly Weather Review*, *1390*(12), 3781–3797, doi:10.1175/MWR-D-11-00007.1.

Barenblatt, G., and G. Golitsyn (1974), Local structure of mature dust storms, *J. Atmos. Sci.*, *310*(7), 1917–1933.

Barenblatt, G. I., A. J. Chorin, and V. M. Prostokishin (2005), A note concerning the Lighthill "sandwich model" of tropical cyclones, *Proc. Natl. Acad. Sci. U.S.A.*, *1020*(32), 11148–11150, doi:10.1073/pnas.0505209102.

Bell, M., M. Montgomery, and K. Emanuel (2012), Air-sea enthalpy and momentum exchange at major hurricane wind speeds observed during CBLAST, *J. Atmos. Sci.*, doi:10.1175/JAS-D-11-0276.1.

Donelan, M., B. K. Haus, N. Reul, W. J. Plant, M. Stiassnie, H. C. Graber, O. B. Brown, and E. S. Saltzman (2004), On the limiting aerodynamic roughness of the ocean in very strong winds, *Geophys. Res. Lett.*, *31*, L18306, doi:10.1029/2004GL019460.

Emanuel, K. A. (1995), Sensitivity of tropical cyclones to surface exchange coefficients and a revised steady-state model incorporating eye dynamics, *J. Atmos. Sci.*, *520*(22), 3969–3976.

Fairall, C. W., M. L. Banner, W. L. Peirson, W. Asher, and R. P. Morison (2009), Investigation of the physical scaling of sea spray spume droplet production, *J. Geophys. Res.*, *1140*(C10), 1–19, doi:10.1029/2008JC004918.

French, J. R., W. M. Drennan, J. A. Zhang, and P. G. Black (2007), Turbulent fluxes in the hurricane boundary layer part I: Momentum flux, *J. Atmos. Sci.*, *640*(4), 1089–1102, doi:10.1175/JAS3887.1.

Holthuijsen, L. H., M. D. Powell, and J. D. Pietrzak (2012), Wind and waves in extreme hurricanes, *J. Geophys. Res.*, *117*, C09003, doi:10.1029/2012JC007983.

Kudryavtsev, V. (2006), On the effect of sea drops on the atmospheric boundary layer, *J. Geophys. Res.*, *111*, C07020, doi:10.1029/2005JC002970.

Kudryavtsev, V. N., and V. K. Makin (2011), Impact of ocean spray on the dynamics of the marine atmospheric boundary layer, *Boundary-Layer Meteorology*, *1400*(3), 383–410, doi:10.1007/s10546-011-9624-2.

Large,W., and S. Pond (1981), Open ocean momentum flux measurements in moderate to strong winds, *J. Phys. Oceanogr.*, *11*, 324–336.

Makin, V. (2005), A note on the drag of the sea surface at hurricane winds, *Boundary-Layer Meteorology*, *115*, 169–176, doi:10.1007/s10546-004-3647-x.

Mueller, J. A., and F. Veron (2009), Nonlinear formulation of the bulk surface stress over breaking waves: Feedback mechanisms from air-flow separation, *Boundary-Layer Meteorology*, *1300*(1), 117–134, doi:10.1007/s10546-008-9334-6.

Pielke, R. A., and T. J. Lee (1991), Influence of sea spray and rainfall on the surface wind profile during conditions of strong winds, *Boundary-Layer Meteorology*, *550*(3), 305–308, doi:10.1007/BF00122582.

Powell, M. D., P. J. Vickery, and T. A. Reinhold (2003), Reduced drag coefficient for high wind speeds in tropical cyclones, *Nature*, *422*, 279–83, doi:10.1038/nature01481.

Richter, D. H., and P. P. Sullivan (2013), Momentum transfer in a turbulent, particle-laden Couette flow, *Physics of Fluids*, in review.